

Directivity and Sound Power Radiated by a Source Under a Boundary Layer

M. G. Smith* and C. L. Morfey†

University of Southampton, Southampton, SO17 1BJ England, United Kingdom

DOI: 10.2514/1.19138

This paper considers the radiation of sound from compact 2-D or 3-D sources located in an otherwise rigid wall, bounding a region of fluid flowing parallel to the wall. The sound radiation problem is modeled using a wave number decomposition. Numerical results show how the radiated power and directivity depend on the freestream flow Mach number and the thickness of the boundary layer adjacent to the wall. The numerical model is validated by comparing the sound power and directivity obtained in the limiting case of a thin boundary layer with that obtained from an alternative analytical model in which the flow is uniform and there is slip at the boundary.

Nomenclature

c_0	=	speed of sound
D	=	operator $\partial/\partial t + \mathbf{U} \cdot \nabla$, which Fourier transforms to $j(\omega - k_x U)$
k	=	acoustic wave number, ω/c_0
k_x, k_y, k_z	=	wave numbers in the x and y directions and in the z direction in the region of uniform flow
M_∞	=	Mach number in the region of uniform flow
$p(x, y, z, t)$	=	acoustic pressure field
$\tilde{p}(k_x, k_y, z)$	=	acoustic pressure at a single frequency, Fourier-transformed to wave number domain in the x and y coordinates
q	=	particle displacement in the wall-normal direction
\mathbf{U}	=	mean velocity vector
$U(z)$	=	velocity profile in the parallel mean flow
U_∞	=	mean flow velocity in the region of uniform flow
\mathbf{u}	=	acoustic particle velocity vector
(u_x, u_y, u_z)	=	components of the acoustic particle velocity vector
W_{rad}	=	radiated power
Z_{rad}	=	radiation impedance
ρ_0	=	local fluid density
χ	=	displacement impedance, \tilde{p}/\tilde{q}
ω	=	angular frequency,

I. Introduction

MOST attempts to model the sound field of sources radiating into a moving fluid have involved the assumption of uniform flow: this applies whether the sources are located in the body of a fluid [1] or at a wall [2–5]. Real flows have a boundary layer next to bounding surfaces and this may be expected to modify the radiation characteristics of a source in the surface. The effect of a boundary layer was considered by Dowling [6] in estimating low wave number sound radiated by turbulence in a low Mach number flow, but the present approach is more general; it allows the sound field in the fluid to be calculated for all wave numbers and for arbitrary Mach number profiles and boundary-layer thicknesses.

The specific problem considered here is shown in Fig. 1. A 2-D or 3-D source radiates into a parallel flow comprising a boundary layer

Presented as Paper 3014 at the 10th AIAA/CEAS Aeroacoustics Conference, Manchester, United Kingdom; received 26 July 2005; revision received 28 April 2006; accepted for publication 15 May 2006. Copies of this paper may be made for personal or internal use, on condition that the copier pay the \$10.00 per-copy fee to the Copyright Clearance Center, Inc., 222 Rosewood Drive, Danvers, MA 01923; include the code \$10.00 in correspondence with the CCC.

*Technical Manager, Institute of Sound and Vibration Consulting; mgs@isvr.soton.ac.uk.

†Professor Emeritus, Institute of Sound and Vibration.

and a semi-infinite region of uniformly flowing fluid. The aim is to show how the source directivity and sound power radiation are influenced by the freestream flow Mach number and the thickness of the boundary layer.

Although results are presented specifically for compact surface-displacement sources, the method of solution can be applied to other problems involving sound radiation in the presence of a boundary layer, such as radiation from noncompact displacement sources at a wall (e.g., vibrating plates) or radiation due to fluctuating body forces on the fluid (e.g., sources of aerodynamic noise arising from turbulent flow over the surface). The methods described in this paper are thus potentially relevant to a range of aeroacoustic problems; examples include active noise control systems in aeroengine intake ducts, aerodynamic noise sources on airfoils, and the radiation damping of vibrating airframe panels.

II. Governing Equations

In the analysis that follows, the governing equations for sound propagation in a parallel shear flow at a discrete wave number are derived from the Euler equations for an inviscid fluid. The linearized momentum and continuity equations in vector notation, for small amplitude perturbations of the parallel shear flow in Fig. 1, are [7]

$$\rho_0(\bar{D}\mathbf{u} + (\mathbf{u} \cdot \nabla)\mathbf{U}) = -\nabla p \quad (1)$$

$$\frac{1}{\rho_0 c_0^2} \bar{D}p = -\nabla \cdot \mathbf{u} \quad (2)$$

where \mathbf{U} is assumed to have the form $\mathbf{U} = [U(z), 0, 0]$, \mathbf{u} has components (u_x, u_y, u_z) , and p is acoustic pressure. The unperturbed values of local fluid density ρ_0 and speed of sound are both allowed to be functions of z in this derivation, but are taken as constant in the numerical examples. \bar{D} is the operator $\partial/\partial t + \mathbf{U} \cdot \nabla$.

Because of the assumed form of the mean flow, Eqs. (1) and (2) are homogeneous in the three time/space variables t , x , and y and may be Fourier-transformed to the frequency/wave number variables ω , k_x , and k_y . The convention used for the transform is that solutions of the following form are sought:

$$p(x, y, z, t) = \tilde{p}(k_x, k_y, z) e^{j(\omega t - k_x x - k_y y)} \quad (3)$$

Other acoustic variables may be similarly transformed. In what follows, the tilde denoting a transformed variable will be dropped for clarity. Also, because solutions for these transformed variables will be sought for constant k_x and k_y , the partial derivatives may be replaced by ordinary derivatives.

The theory given here is general and applies to 3-D problems; the equivalent expressions for the 2-D case are obtained by setting $k_y = 0$, and their numerical implementation requires a single rather

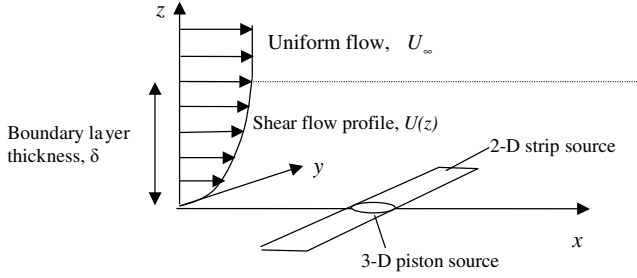


Fig. 1 Boundary-layer flow in the x direction over a surface at $z = 0$ with either a piston or strip source.

than double spatial Fourier transform. For computational and presentational reasons, most of the results shown are for 2-D problems.

Fourier transformation of Eqs. (1) and (2) provides a set of four simultaneous equations that may be solved for the four acoustic variables u_x , u_y , u_z and p :

$$\rho_0 \left(\bar{D} u_x + u_z \frac{dU}{dz} \right) = j k_x p \quad (4)$$

$$\rho_0 \bar{D} u_y = j k_y p \quad (5)$$

$$\rho_0 \bar{D} u_z = - \frac{dp}{dz} \quad (6)$$

$$\frac{1}{\rho_0 c_0^2} \bar{D} p = j k_x u_x + j k_y u_y - \frac{d u_z}{dz} \quad (7)$$

where the Fourier transform of \bar{D} is given by

$$\bar{D} = j(\omega - k_x U) \quad (8)$$

Using Eqs. (4) and (5) to eliminate u_x and u_y from Eq. (7), and leaving Eq. (6) unchanged, leads to the following coupled equations in u_z and p :

$$\frac{d u_z}{dz} = - \frac{1}{\rho_0 \bar{D}} \left[\left(\frac{\bar{D}^2}{c_0^2} + k_x^2 + k_y^2 \right) p + j k_x \rho_0 u_z \frac{dU}{dz} \right] \quad (9)$$

$$\frac{dp}{dz} = - \rho_0 \bar{D} u_z \quad (10)$$

Combining the z derivative of Eq. (10) with Eqs. (8) and (9) to eliminate u_z and $d u_z / dz$ leads directly to the second-order differential equation in p derived by Pridmore–Brown [8].

These equations are difficult to solve for two reasons. Firstly, for the sound radiation problem, a solution is, in principle, required for all values of k_x . However, from Eq. (8) it may be seen that for $k_x > \omega / U_\infty$ or, equivalently, for $k_x / k > c_0 / U_\infty$, \bar{D} becomes zero at some point through the boundary layer (a critical layer [9,10]). When this happens, Eq. (9) appears to have a singularity, although actually it may be shown that the equations remain finite [11]. Secondly, Eq. (9) requires the evaluation of the mean velocity derivative dU/dz , which can become infinite in some circumstances, for example, at the wall if a $1/7$ power law profile is used to model a turbulent boundary layer or when the boundary-layer thickness is allowed to become small (i.e., the limiting case of a uniform flow with slip at the boundary).

Useful alternative equations that largely circumvent these problems are obtained by using either the normal particle

displacement $q = u_z / \bar{D}$ or the “displacement impedance” $\chi = p/q = \bar{D} p / u_z$ as variables, in place of particle velocity u_z .

Differentiating q with respect to z and using Eq. (9) to eliminate $d u_z / dz$ leads to the following simultaneous equations for q and p :

$$\frac{dq}{dz} = - \frac{1}{\rho_0 \bar{D}^2} \left(\frac{\bar{D}^2}{c_0^2} + k_x^2 + k_y^2 \right) p \quad (11)$$

$$\frac{dp}{dz} = - \rho_0 \bar{D}^2 q \quad (12)$$

These equations do not involve the mean velocity gradient, but Eq. (11) does have a singularity when \bar{D} becomes zero. Continuity of particle displacement across a thin shear layer may be derived directly from Eq. (11) providing \bar{D} is not zero anywhere within the layer. At wave numbers where a critical layer occurs, however, dq/dz becomes infinite and q becomes discontinuous across the layer.

Alternatively, differentiating χ with respect to z and using Eq. (11) to eliminate dq/dz leads to the following governing differential equations for χ and p :

$$\frac{d\chi}{dz} = \frac{1}{\rho_0} \left(\frac{\bar{D}^2}{c_0^2} + k_x^2 + k_y^2 \right) \left(\frac{\chi}{\bar{D}} \right)^2 - \rho_0 \bar{D}^2 \quad (13)$$

$$\frac{dp}{dz} = - \rho_0 \bar{D}^2 \frac{p}{\chi} \quad (14)$$

It can be shown that these equations do not have a singularity at a critical layer, because χ / \bar{D} remains finite as \bar{D} tend to zero [11]. They also have the advantage of not involving dU/dz .

To solve the radiation problem for outgoing waves using Eqs. (13) and (14), initial values for χ and p are specified at the edge of the boundary layer in the uniform flow, and the equations are used to integrate through the boundary layer to the wall. An arbitrary value of $p = 1$ may be used for the pressure. The initial value for χ in the mean flow is obtained by setting $d\chi/dz = 0$ in Eq. (13), as required for outgoing waves in the uniform flow region, to give

$$\chi = \frac{-j \rho_0 \bar{D}^2}{k_z} \quad (15)$$

where the appropriate square root is selected by choosing k_z , the wave number component in the z direction for the outgoing wave in the region of uniform flow, to be given by

$$j k_z = \sqrt{k_x^2 + k_y^2 - (\omega - k_x U_\infty)^2 / c_0^2} \quad (16)$$

For sufficiently large k_x and k_y , k_z becomes imaginary: waves are cut off in the region of uniform flow and decay away from the surface. In the uniform flow, outgoing waves can propagate and carry energy only for values of k_x and k_y that lie inside the ellipse defined by

$$\left(\frac{k_x}{k} \right)^2 + \left(\frac{k_y}{k} \right)^2 = \left(1 - \frac{k_x}{k} M_\infty \right)^2 \quad (17)$$

III. Sound Radiation from a Vibrating Surface

In this section, sound radiated by a source under a boundary layer is modeled using a wave number decomposition of the vibrating surface. Solving Eqs. (13) and (14) by integration through the boundary layer gives solutions $p(k_x, k_y, z)$ and $\chi(k_x, k_y, z)$, for any required values of k_x and k_y , based on the arbitrary initial value of $p = 1$ at $z = \delta$. The solution for p must then be normalized to give the particular solution that also satisfies the boundary condition at the vibrating wall.

For the 2-D solutions presented here, the equations were integrated using a fourth-order Runge–Kutta routine in MATLAB, with the error tolerance parameter adjusted to ensure good convergence of the solutions. For 3-D problems, the numerical integration for each wave number pair was carried out using a FORTRAN subprogram based on an International Mathematical and Statistical Library (IMSL) Runge–Kutta–Verner fifth-order and sixth-order routine; this method gave much faster computation times, but required care to ensure that correct solutions were obtained when integrating through a critical layer.

The wall velocity distribution $u_w(x, y)$ is transformed to give its wave number spectrum $u_w(k_x, k_y)$; for a point source located at (x_0, y_0) , this is given by

$$u_w(k_x, k_y) = e^{j(k_x x_0 + k_y y_0)} \quad (18)$$

Unit amplitude is assumed for convenience in Eq. (18); the amplitude is normalized out in the results presented next. In terms of the radiation impedance of the surface and the given wall velocity, the required particular solution must satisfy

$$p(k_x, k_y, 0) = u_w(k_x, k_y) Z_{\text{rad}}(k_x, k_y) \quad (19)$$

where the radiation impedance of the surface is given from the displacement impedance at the wall by

$$Z_{\text{rad}}(k_x, k_y) = \frac{\chi(k_x, k_y, 0)}{j\omega} \quad (20)$$

Outside the boundary layer $z > \delta$, the pressure is related to the value at $z = \delta$ via

$$p(k_x, k_y, z) = p(k_x, k_y, \delta) e^{-jk_z(z-\delta)} \quad (21)$$

where k_z is given by Eq. (16).

The complex amplitude of the radiated pressure field $p(x, y, z)$ and the radiated sound power W_{rad} may be obtained from the following inverse Fourier transforms [12].

$$p(x, y, z) = \frac{1}{(2\pi)^2} \iint p(k_x, k_y, z) e^{-j(k_x x + k_y y)} dk_x dk_y \quad (22)$$

$$W_{\text{rad}} = \frac{1}{2(2\pi)^2} \iint \text{Re}[Z_{\text{rad}}(k_x, k_y)] |u_w(k_x, k_y)|^2 dk_x dk_y \quad (23)$$

The double integral in Eq. (22) extends over all wave numbers, and a numerical solution must be truncated somewhere outside the ellipse defined by Eq. (17). This truncation limits the accuracy with which the sound field in the immediate vicinity of the source can be resolved. This limitation does not apply to Eq. (23), because $\text{Re}[Z_{\text{rad}}(k_x, k_y)]$ is zero outside the ellipse.

The integrands in Eqs. (22) and (23) may also only be evaluated at a finite number of wave number points. In the solutions presented here, the continuous Fourier transforms were approximated by discrete fast Fourier transforms in MATLAB using equally spaced wave number values. The discretization implies a periodic source, with image sources outside the spatial region of interest that perturb the sound field near the edge of the main spatial domain. Accurate solutions in the region around the true source were obtained by calculating the integrand for a large number of closely spaced wave number values to give a solution over a correspondingly large spatial domain, thus pushing the image sources further away. For example, for a 2-D problem with $M_\infty = 0.3$, 8192 points in the range $-3 < k_x/k_0 < 3$ were used. Some damping was also included by giving the speed of sound a small imaginary part; this helped to suppress the effect of image sources and other inaccuracies caused by the peaks in radiation impedance near coincidence that are discussed in the next section.

In any implementation of this method it should be noted that FFT routines commonly assume a Fourier decomposition based on the opposite sign convention to Eq. (22). This means that the evaluation

of the inverse transform in Eq. (22) actually requires the forward FFT routine to be used, and use of an inverse FFT routine leads to a solution that is flipped in the spatial domain.

In Eq. (23) it is assumed that power is conserved as the sound propagates through the boundary layer. This issue is not trivial [11,13] and will be demonstrated in a separate publication.

IV. Radiation Impedance and Radiated Power

This section considers the sound power radiated by a source, first for the case where the boundary-layer thickness shown in Fig. 1 is taken to be infinitesimally small and then with the effect of a finite boundary-layer thickness included using the method set out in the previous sections.

A. Zero Boundary-Layer Thickness, $\delta/\lambda = 0$

For a uniform flow with slip past the wall, a simple 3-D extension of the expressions given by Morse and Ingard [1] shows that the radiation impedance of the surface may be written

$$Z_{\text{rad}}(k_x, k_y) = \frac{j\rho c(\omega - U_\infty k_x)^2}{\omega \sqrt{c^2(k_x^2 + k_y^2) - (\omega - U_\infty k_x)^2}} \quad (24)$$

The real part of the radiation impedance normalized by ρc defines the radiation efficiency of the wall at a single wave number. This quantity for a uniform 0.6 M number flow is plotted as a solid line in Fig. 2 as a function of k_x ; k_y is zero here. Coincidence peaks occur at

$$\frac{k_x}{k} = \frac{\pm 1}{(1 \pm M_\infty)}$$

and waves propagating upstream (negative k_x) are generally radiated more efficiently than those propagating downstream.

Noting that $\text{Re}(Z_{\text{rad}})$ is only nonzero inside the ellipse defined by Eq. (17) and also that, from Eq. (18), $|u_w| = 1$ for all k_x and k_y , Eq. (23) gives the radiated power as

$$W_{\text{rad}} = \frac{1}{2(2\pi)^2} \int_{-k/(1+M_\infty)}^{k/(1+M_\infty)} \int_{-k_y}^{k_y} \frac{j\rho c(\omega - U_\infty k_x)^2}{\omega \sqrt{c^2(k_x^2 + k_y^2) - (\omega - U_\infty k_x)^2}} dk_y dk_x \quad (25)$$

where

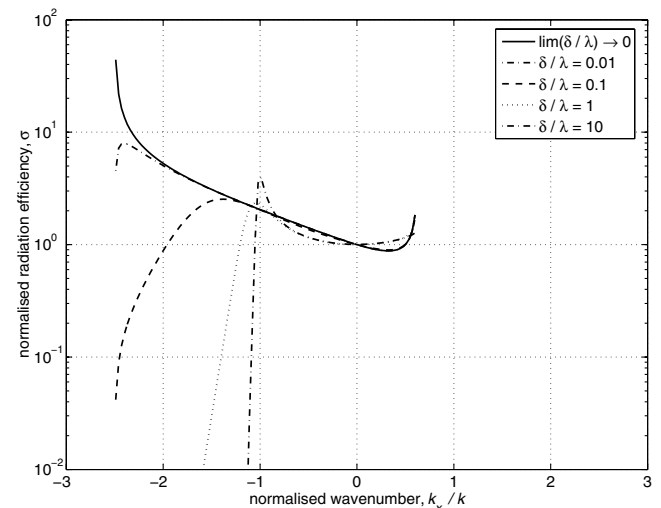


Fig. 2 Radiation efficiency at $M_\infty = 0.6$ for four values of δ/λ and for uniform flow. Radiation efficiency is zero outside the range shown; $k_y = 0$.

$$\frac{k_{y1}}{k} = \sqrt{\left(1 - \frac{k_x}{k} M_\infty\right)^2 - \left(\frac{k_x}{k}\right)^2}$$

Equation (25) is difficult to evaluate analytically, but alternative derivations for the 2-D and 3-D problems have been published by Leppington and Levine [2] and Levine [3]. They show that, relative to no flow, the power of a compact source radiating into a uniform flow of Mach number M_∞ , $W(M_\infty)$, is given by

(2-D line source)

$$\frac{W(M_\infty)}{W(0)} = \frac{1 + (1/2)M_\infty^2}{(1 - M_\infty^2)^{5/2}} \quad (26)$$

(3-D point source)

$$\frac{W(M_\infty)}{W(0)} = \frac{1 + (1/3)M_\infty^2}{(1 - M_\infty^2)^3} \quad (27)$$

Figure 3 compares plots of these expressions with the results of numerical integration of Eq. (25). As expected, because both methods are exact, there is perfect agreement between the spatial domain and wave number domain solutions.

B. Arbitrary Boundary-Layer Thickness, $\delta/\lambda > 0$

The case of boundary layers of finite thickness is now considered. Here the radiation impedance is obtained by numerical integration of Eq. (13) through the boundary layer for each wave number. Figure 2 shows the effect on the real part of the radiation impedance of boundary layers varying from 0.01 to 10 wavelengths thick. Components propagating upstream with wave numbers in the range $1/(1 - M_\infty) < k_x/k < -1$ are strongly affected by the boundary layer; these waves are cut on in the uniform external flow but cut off at the wall and have to tunnel through the boundary layer. It is interesting to note that waves propagating downstream with

$$\frac{1}{(1 + M_\infty)} < \frac{k_x}{k} < 1$$

are cut off independently of the boundary-layer thickness, because power can never propagate in the region of uniform flow and the real part of the radiation impedance is thus always zero in this range of wave numbers.

Figure 4 shows, for the 2-D case, the effect of the increasing boundary-layer thickness on the power radiation of a line source. The effect of the flow in increasing the power output is reduced as δ/λ increases, and for a boundary layer one wavelength thick, the power of the source is virtually independent of the Mach number.

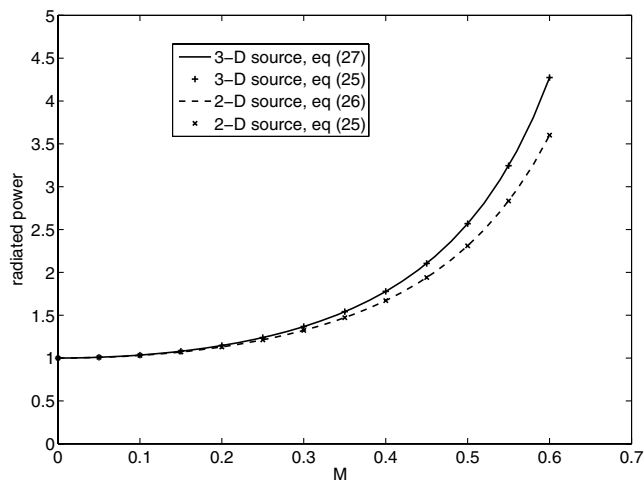


Fig. 3 Power radiated into a uniform flow from 2-D and 3-D compact sources as a function of Mach number; comparison of analytical solutions using Eqs. (26) and (27) (lines) and numerical integral results based on Eq. (25).

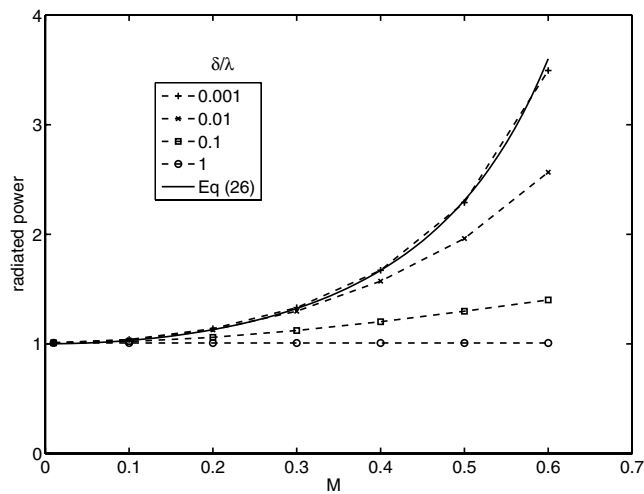


Fig. 4 Power radiated from a 2-D line source as a function of Mach number and nondimensional boundary-layer thickness δ/λ . The solid line shows the analytical result [Eq. (26)]; dotted lines and symbols show numerical results.

V. Radiated Pressure Field

Before examining the effect of nonuniform flow, it is useful to consider the far-field pressure produced by a source radiating into a uniform flow. This may be obtained by numerically evaluating Eq. (22) using the solutions obtained from Eqs. (19) and (21). For a 2-D case, this means evaluating

$$p(x, z) = \frac{1}{2\pi} \int (u_w(k_x) Z_{\text{rad}}(k_x) e^{-jk_z z}) e^{-jk_x x} dk_x \quad (28)$$

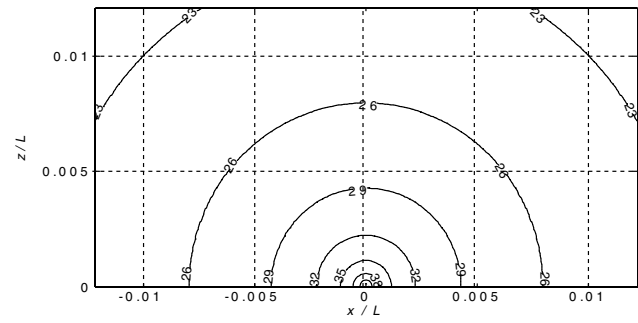
where the radiation impedance is given by Eq. (24), the source wave number spectrum, $u_w(k_x)$, is given by Eq. (18), and the z wave number, k_z , is given by Eq. (16); k_y is set to zero in each case.

Figure 5 shows the effect of a 0.3 M number uniform flow over a line source as predicted by Eq. (28). The zero flow case, Fig. 5a, shows the expected cylindrical spreading, with the 3 dB contour separation distance progressively doubling as expected for this 2-D problem. In the presence of flow (Fig. 5b), convective amplification increases the sound pressure level upstream and decreases the level downstream relative to the no-flow levels.

For nonuniform flow, the sound field is obtained by evaluating Eq. (22) numerically, using the solutions obtained from the numerical integration of Eqs. (13) and (14). The effect of boundary layers 0.1 and 1.0 wavelengths thick is shown in Figs. 6a and 6b. Compared with the uniform flow solution in Fig. 5b, the effect of convective amplification is modified in the upstream direction by refraction of sound away from the surface to create a shadow zone, and in the downstream direction the sound pressure is increased due to channeling of the sound by the boundary layer.

Figures 5 and 6 show the effect of a boundary layer on the pressure field in the x - z plane for 2-D sources; similar effects can be shown for 3-D sources. Because plotting a full 3-D solution is not practicable, Fig. 7 shows, as an example, the pressure field in the x - y plane at the wall, $z = 0$, for a point source under a boundary layer one wavelength thick. In the immediate vicinity of the source, the pressure contours are approximately circular, as for the zero flow case, but at larger distances, the shadow zone upstream and the downstream channeling of sound are apparent.

As noted in the Introduction, the method described in this paper may be applied to noncompact sources. As an example, Fig. 8 shows the sound field radiated by a 2-D piston source with nondimensional width of $ka = 6.25$. In the absence of flow, a source of this size radiates a primary lobe normal to the surface and has a single side lobe on either side of the primary lobe [14]. Figure 8 shows that the effect of a flow with a very thin boundary layer is to direct the primary lobe in the downstream direction and to produce a second side lobe in the upstream direction.



- [6] Dowling, A. P., "Mean Flow Effects on the Low-Wave Number Pressure Spectrum on a Flexible Surface," *Journal of Fluids Engineering*, Vol. 108, No. 1, 1986, pp. 104–108.
- [7] Goldstein, M. E., *Aeroacoustics*, McGraw-Hill, New York, 1976.
- [8] Pridmore-Brown, D. C., "Sound Propagating in a Fluid Flowing Through an Attenuating Duct," *Journal of Fluid Mechanics*, Vol. 4, Aug. 1958, pp. 393–406.
- [9] Campos, L. M. B. C., Oliveira, J. M. G. S., and Kobayashi, M. K., "On Sound Propagation in a Linear Shear Flow," *Journal of Sound and Vibration*, Vol. 219, No. 5, 1999, pp. 739–770.
- [10] Tam, C. K. W., and Morris, P. J., "The Radiation of Sound by the Instability Waves of a Compressible Plane Turbulent Shear Layer," *Journal of Fluid Mechanics*, Vol. 98, Part 2, 1980, pp. 349–381.
- [11] Smith, M. G., "Sound Radiation from a Vibrating Surface Under a Boundary Layer," Ph.D. Thesis, Inst. of Sound and Vibration Research, Univ. of Southampton, Southampton, England, U.K., 2004.
- [12] Cremer, L., Heckl, M., and Ungar, E. E., *Structure-Borne Sound*, Springer-Verlag, Berlin, 1973.
- [13] Morfey, C. L., "Acoustic Energy in Non-Uniform Flows," *Journal of Sound and Vibration*, Vol. 14, No. 2, 1971, pp. 159–170.
- [14] Pierce, A. D., *Acoustics: An Introduction to Its Physical Principles and Applications*, Acoustical Society of America, Melville, NY, 1989.

C. Bailly
Associate Editor